Supplementary Material for : Temperature effect on ionic current and ssDNA transport through nanopores

L. Payet, M. Martinho, C. Merstorf, M. Pastoriza-Gallego, J. Pelta, V. Viasnoff, L. Auvray, M. Muthukumar and J. Mathé

Material and Methods

The toxin Aerolysin was synthetized using the following procedure. We have transformed E. coli BL21 strain with the plasmid containing proaerolysin sequence. This plasmid is endowed with different elements for production and purification of the protein: inducible expression with IPTG system, signal for periplasmic localization, histidine tag in C-terminal region of the protein. The recombinant proaerolysin protein is purified by an affinity chromatography of histidine-tagged proteins (His Spin Trap, Amersham). The purity of the preparation is determined by densitometry analysis of Coomassie blue SDS-polyacrylamide gel electrophoresis, to 99 $\pm$ 1% (w/w). The propeptid of pro-AL monomeres are stored at a final concentration of 0.4 g/l in water. Upon use, the propeptid is first cut by some Trypsin at a final concentration of 0.36 μM in water. The active AL monomers were then diluted in the buffer to a ratio of 10 μl of this solution per milliliter of buffer in the cis chamber.

The current-Voltage curves of a single pore were measured by applying a triangle voltage between -150 mV and +150 mV and a rate of about 2.3 V/s for 25 cycles. The upward and downward ramps are then averaged to reduce the noise amplitude and discard the capacitive component of the current. The variability from pore to pore are estimated to $\pm$ 7.5 % at 25°C (1). It becomes slightly larger as the temperature is raised. The IV-Curve obviously depends on the orientation of the pore with respect to the electrode polarization. We thus used the following strict insertion procedure. The membrane is formed on a Teflon aperture separating two chambers. The first one is grounded and thereafter called *cis* chamber. The potential (positive or negative) is applied to the second chamber thereafter called *trans* chamber. The toxin monomers are inserted in the *cis* chamber after the formation of the lipid bilayer. The bilayer is never reformed while waiting for a pore insertion. Therefore it is very likely to observe insertion of the toxin with its extra-membrane part in the cis (grounded) chamber. Indeed, using all pores insertions observed for the present data set, 92% of the α-HL insertions (173 over 187) and 90% (88 over 97) of the AL insertions had a I-V curve oriented as in Figure 1 of the article.

The translocation events are captured on the fly using the analog triggering of the acquisition board. The trigger threshold was set to 90% of the empty pore current at the voltage studied. From these events we extract the open pore current the blocked current the dwell time and the inter event time. The very short events are smoothed by the low pass filter altering the dwell time and the blocked pore (as explained in (2–4)). In order to perform the analysis of the events, a second current threshold is applied which discard the noisy spikes and allows a better definition of the time scales and blocked current. This threshold is defined from the all-point histogram of the current traces of all the event and is set at the end of the open pore current peak. We represent the result of an experiment for a certain set of parameters (pore, voltage and temperature) by a two dimensional histogram (like Figures S-2 and S-6) allowing to distinguish easily clusters of events of different kind as the 3' and 5' clouds previously reported (5, 6) for forward and backward threading of a ssDNA in α-Hemolysin.

IV Curves calculation

Following (7), we calculated the IV curves at different temperature and deduced the asymmetry. We first calculated the electrostatic potential seen by the ions at different applied voltage (see Figure S 1 for a voltage of -120 mV) and then the IV curve itself. Resolving the 1D Nerst-Planck equation numerically (1, 8). Table S-T 1 references the amino acid position and calculated electric potential at the center of the pore. These values are very close to the one used for α-Hemolysin in Ref (7). The mean diameter of the channel used in the calculation was 1.6 nm for αHL and 1.4 nm for AL.

α-Hemolysin				Aerolysin			
Amino Acid	Position	pK	potential (mV)	Amino Acid	Position	pK	potential (mV)
E111	0.05	4.5	-18.8	K238	0.06	10.5	+17.1
K147	0.13	10.5	+13.5	E258	0.37	4.5	-23.9
D127	0.77	3.9	-18.1	K242	0.46	10.5	+17.1
K131	0.83	10.5	+13.5	K244	0.69	10.5	+17.1
D128	0.91	3.9	-18.1	E258	0.78	4.5	-23.9
				K246	0.90	10.5	+17.1
				E252	0.95	4.5	-23.9

Figure S-T 1: Amino acid positions and potential along the pore axis for α-Hemolysin and Aerolysin. The potential was calculated for a cylindrical pore of diameter 16 and 14 Å for α-Hemolysin and Aerolysin respectively. The position along the pore axis are given as fraction of the pore length. The pore length is 5 nm for both pore, the Debye length is 3 Å and the pH of the buffer is 7.5 .

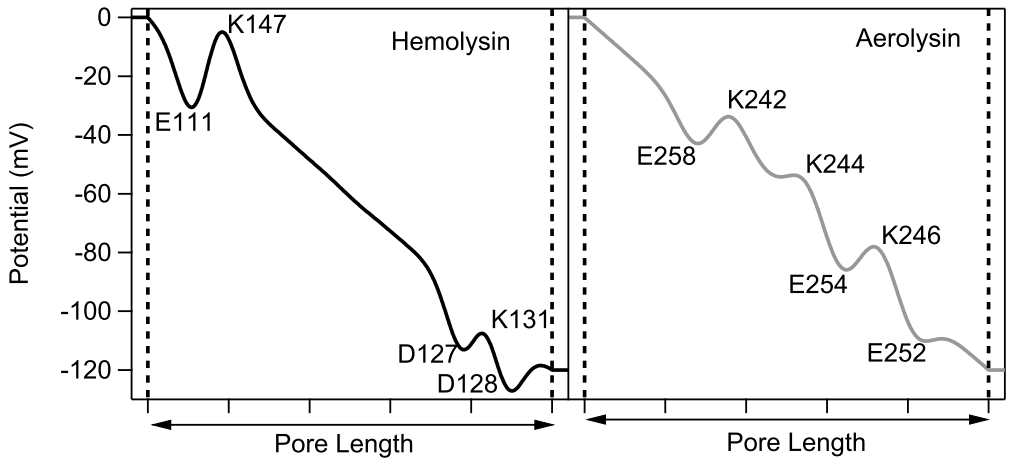

Figure S- 1: Electrostatic potential map along the pore axis due to the voltage applied (-120 mV here) and to the charge of the amino acids present in the pore channel. We discarded the extra membranar part of the toxins as the main features in the IV curves depends on the barrel charges (1, 9).

ssDNA transport

We represent the measurements as a two dimensional probability density function $P(I_b, T_t)$ of events in order to discriminates clusters of event of different kind. In Figure S-2, we display the P distribution at room temperature and for 4 voltages for Aerolysin pores. Two types of events are observed: Short time events ($\sim 100\,\mu$s) associated with DNA bumping the pore without full insertion and longer duration events (~ 1 ms) associated to molecules inserted in the pore constriction. Indeed the shorter time increases with voltage indicating that the DNA molecules are blocked at the entrance of the pore. The unblocking would occur by diffusion out of the pore entrance region while the voltage forces the molecules to stay in the pore (10). At about 100 mV, the longer time events are observed and their duration decreases with the applied voltage indicating that the molecule goes fully in the pore. Using PCR DNA molecules with a different sequence were proved to pass through AL pore (11).

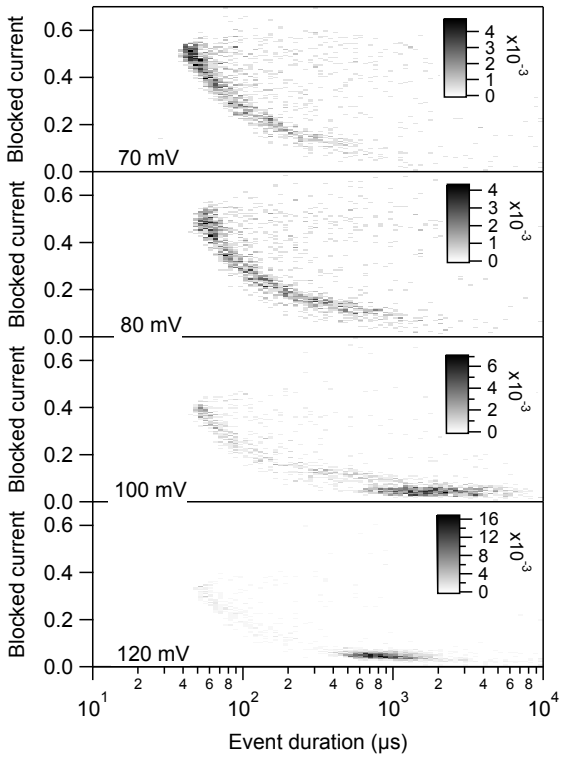

Figure S- 2: Two dimensional probability density function $P(Ib, Tt)$ of events in Aerolysin at room temperature and at voltages of 70 mV 80 mV 100 mV and 120 mV. The increase of the normalized blocked current for the shorter time is due to the low pass filtering of the signal as described in (3, 4). The number of events in each histograms are 1916, 1883, 1889 and 1875 for 70, 80, 100 and 120 mV respectively.

The figure 3 shows the frequency of events per μM of molecules in αHL and AL as a function of voltage at a constant temperature T=10°C. As expected for both nanopores, the frequency increases with voltage.

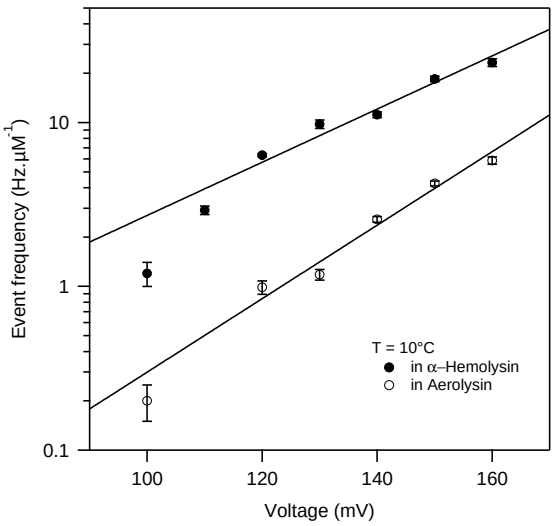

Figure S- 3: Event frequency measured at T=10°C for different voltages using α-Hemolysin (filled circles) and Aerolysin (empty circles). The plain curves are exponential fits leading to an effective charge of about $1.5e$. From the extrapolation at zero voltage and using barrier crossing formalism as in (12) we obtain a free energy barrier of about 10 k_BT.

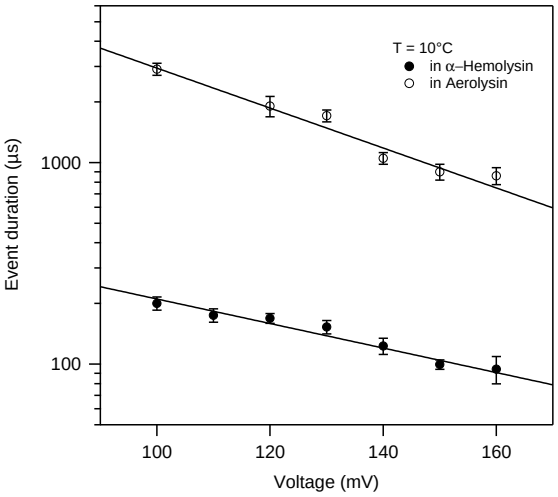

Figure S- 4: Event duration measured at T=10°C for different voltages using α-Hemolysin (filled circles) and Aerolysin (empty circles). Plain curves are exponential fits leading to effective charges of $0.4e$ in α-Hemolysin and $0.6e$ in Aerolysin, very similar to the ones obtained for other polyelectrolytes in Ref. (13–15).

The reaction-rate theory predicts that the variation of the translocation rate with temperature and voltage follows this relation:

$$F_e(V,T) = f_0 e^{\frac{-\Delta F^*}{kT}} e^{\frac{q_f V}{k_B T}} \qquad (1)$$

where ΔF^* is the entrance energy barrier defined in the main text, V is the applied voltage, q_f is the effective charge of the molecule in bulk solution. These exponential dependences describe the translocation of the polymer in a complex energy landscape with an energy barrier probably of enthalpic and entropic origins which decreases with the applied voltage (16).

From the graphs, we can extract the different parameters defined in the above formalism. At constant temperature, the slope of the frequency *vs* voltage in a semi-Log plot yields to a characteristic voltage $V_f = \frac{k_B T}{q_f}$ representing the voltage needed to give to the molecule a energy of $k_B T$. To evaluate ΔF^*, we estimate f_0 proportional to an upper bound for the ssDNA flux to the pore which gives $f_0 \sim CDr$, where D is the bulk diffusion coefficient of the oligomer (about $10^{-7} cm^2.s^{-1}$), C its concentration and r is the radius of the pore. This estimation yields to a barrier of about $10 k_B T$ in both pores.

The values of V_f we obtain for AL and HL at 10 °C are very close to the previously reported ones (12, 17).

Water evaporation

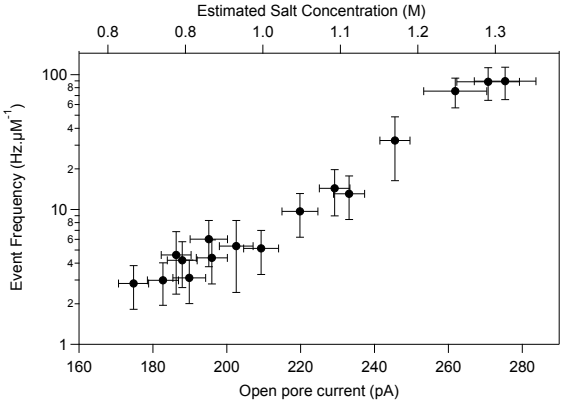

Figure S- 5: Event frequency of entry of ssDNA in αHL pore at $V = 120mV$ and $T = 50°$C. We observe clearly an exponential increase of this frequency as a function of the salt concentration due to water evaporation. The influence of the increase of DNA concentration due to evaporation can be neglected.

We demonstrate on Figure S-5 the absolute necessity to control the water evaporation, in particular at high temperature. Figure S-5 represents the frequency measured with αHL pores thermalized to $T = 50°$C without control of the evaporation. As already observed in (18), the events frequency has an exponential dependence on salt concentration (at high concentration which is the case here). On the other hand, the water evaporation will increase the concentrations of DNA and salt. The influence of the DNA concentration increase being only linear, we therefore observed an exponential dependence of the frequency with the salt concentration. The salt concentration (upper scale on Figure S-5) is deduce from the open pore current considering that the concentration is 1.0 M if the current is equal to the mean open pore current from the Figure 2 of the main paper at the correct temperature. In this case the mean open pore current is 209 pA at (50°).

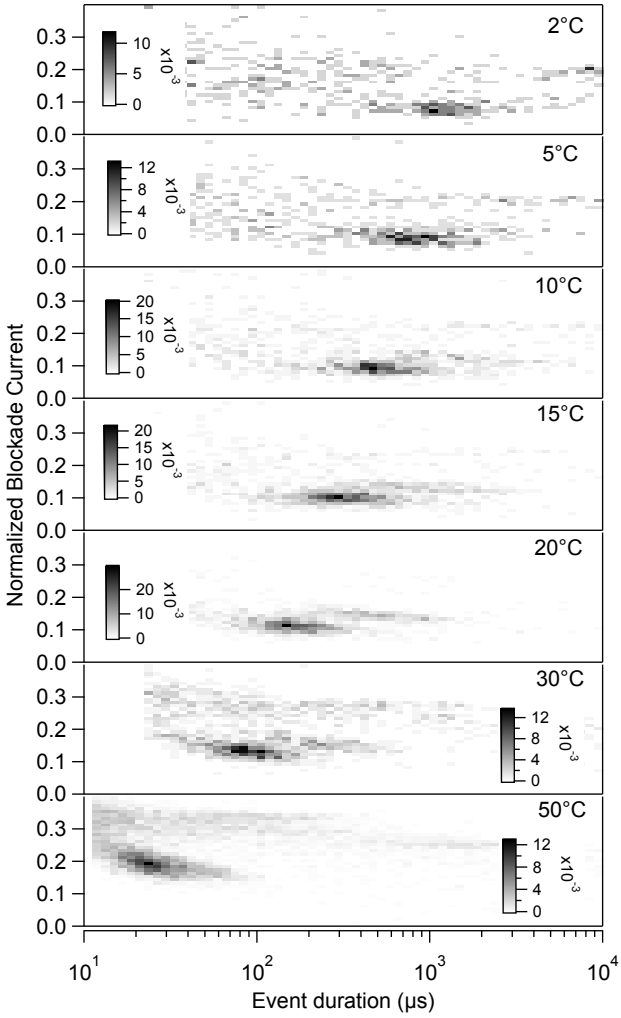

Figure S- 6: Two dimensional probability density functions $P(I_b, T_t)$ of events in α-Hemolysin at $V = 100$ mV and at Temperature ranging from 2 to 50°C. Two main types of events are observed previously associated to 3'-end and 5'-end entrance in the pore. The two types of event have duration deacrising with temperature. At 50°C they cannot be distinguished. The increase of the normalized blocked current for the shorter time is due to the low pass filtering of the signal as described in (3, 4). The number of event in each histogram are 514, 618, 1059, 1267, 1359, 1628 and 6655 for 2, 5, 10, 15, 20, 30 and 50°C respectively.

References

1. S Bhattacharya, L Muzard, Linda Payet, Jérome Mathé, Ulrich Bockelmann, Aleksei Aksimentiev, and Virgile Viasnoff. Rectification of the current in alpha-hemolysin pore depends on the cation type: The alkali series probed by molecular dynamics simulations and experiments. *J Phys Chem C*, 115(10):4255–4264, 2011.
2. D Pedone, M Firnkes, and U Rant. Data analysis of translocation events in nanopore experiments. *Anal Chem*, 81(23):9689–94, Dec 2009.
3. C Merstorf, B Cressiot, M Pastoriza-Gallego, A G Oukhaled, L Bacri, J Gierak, J Pelta, L Auvray, and J Mathé. DNA unzipping and protein unfolding using nanopores. *Methods Mol Biol*, 870:55–75, Jan 2012.
4. L Payet, M Martinho, M Pastoriza-Gallego, J-M Betton, L Auvray, J Pelta, and J Mathé. Thermal unfolding of proteins probed at the single molecule level using nanopores. *Anal Chem*, 84(9):4071–6, May 2012.
5. J Mathé, A Aksimentiev, D R Nelson, K Schulten, and A Meller. Orientation discrimination of single-stranded dna inside the alpha-hemolysin membrane channel. *Proc Natl Acad Sci USA*, 102(35):12377–82, Aug 2005.
6. J Muzard, M Martinho, Jérome Mathé, Ulrich Bockelmann, and Virgile Viasnoff. Dna translocation and unzipping through a nanopore: some geometrical effects. *Biophys J*, 98(10):2170–8, May 2010.
7. M Misakian and J J Kasianowicz. Electrostatic influence on ion transport through the alphahl channel. *J Membr Biol*, 195(3):137–46, Oct 2003.
8. S Matysiak, A Montesi, M Pasquali, A B Kolomeisky, and C Clementi. Dynamics of polymer translocation through nanopores: theory meets experiment. *Phys Rev Lett*, 96(11):118103, Mar 2006.
9. S Yu Noskov, W Im, and B Roux. Ion permeation through the alpha-hemolysin channel: theoretical studies based on brownian dynamics and poisson-nernst-plank electrodiffusion theory. *Biophys J*, 87(4):2299–309, Oct 2004.
10. M Wiggin, C Tropini, V Tabard-Cossa, N N Jetha, and A Marziali. Nonexponential kinetics of dna escape from a-hemolysin nanopores. *Biophys J*, 95(11):5317–5323, Jan 2008.
11. M Pastoriza-Gallego, M-F Breton, F Discala, L Auvray, J-M Betton, and J Pelta. Evidence of Unfolded Protein Translocation through a Protein Nanopore. *ACS Nano*, 8(11):11350–11360, 2014.
12. S E Henrickson, Martin Misakian, B Robertson, and John J Kasianowicz. Driven dna transport into an asymmetric nanometer-scale pore. *Phys Rev Lett*, 85(14):3057–60, Oct 2000.
13. A G Oukhaled, J Mathé, A-L Biance, L Bacri, J-M Betton, D Lairez, J Pelta, and L Auvray. Unfolding of proteins and long transient conformations detected by single nanopore recording. *Phys Rev Lett*, 98(15):158101, Apr 2007.
14. L Brun, M Pastoriza-Gallego, A G Oukhaled, J Mathé, L Bacri, L Auvray, and J Pelta. Dynamics of polyelectrolyte transport through a protein channel as a function of applied voltage. *Phys Rev Lett*, 100(15):158302, Apr 2008.
15. M Pastoriza-Gallego, L Rabah, G Gibrat, B Thiebot, F Gisou van der Goot, L Auvray, J-M Betton, and J Pelta. Dynamics of unfolded protein transport through an aerolysin pore. *J Am Chem Soc*, 133(9):2923–2931, Mar 2011.
16. Y Lansac, P Maiti, and M Glaser. Coarse-grained simulation of polymer translocation through an artificial nanopore. *Polymer*, 45(9):3099–3110, 2004.
17. A Meller and D Branton. Single molecule measurements of dna transport through a nanopore. *Electrophoresis*, 23(16):2583–2591, 2002.
18. D J Bonthuis, J Zhang, B Hornblower, J Mathé, B I Shklovskii, and A Meller. Self-energy-limited ion transport in subnanometer channels. *Phys Rev Lett*, 97(12):128104, 2006.